

## Article

# Influence of a Frame Structure Building Demolition on an Adjacent Subway Tunnel: Monitoring and Analysis

Wei Wang <sup>1,2,\*</sup>, Xianqi Xie <sup>1,2,3</sup>, Fang Yuan <sup>3</sup>, Peng Luo <sup>1,2</sup>, Yue Wu <sup>2</sup>, Changbang Liu <sup>2</sup> and Senlin Nie <sup>3</sup><sup>1</sup> College of Science, Wuhan University of Science and Technology, Wuhan 430065, China<sup>2</sup> Wuhan Explosions & Blasting Co., Ltd., Wuhan 430056, China<sup>3</sup> State Key Laboratory of Precision Blasting, Jiangnan University, Wuhan 430056, China

\* Correspondence: 13545097785@163.com

**Abstract:** In a complex urban environment, the impact of building demolitions by blasting on the structural integrity of nearby metro tunnels is critical. This study systematically analyzed the blasting and demolition process of a building adjacent to a metro tunnel using various monitoring methods, including blasting vibration, dynamic strain, deformation and settlement, pore water pressure, and displacement. The results indicate that the metro tunnel's vibration response can be divided into four stages: notch blasting, notch closure, overall collapse impact, and auxiliary notch blasting. The most significant impact on the tunnel segments occurred during the building's ground impact phase, with a peak particle velocity of 0.57 cm/s. The maximum tensile and compressive stresses induced in the tunnel segments did not exceed 0.4 MPa, well within the safety limits. Displacement and settlement changes in the tunnel structure were less than 1 mm, far below the warning threshold. Additionally, blasting vibrations significantly affected the pore water pressure in the surrounding soil. However, fluctuations caused by ground impact vibrations were minimal, and the pore water pressure quickly returned to its initial level after the blasting concluded. Throughout the process, no adverse effects on the metro tunnel structure were observed.

**Keywords:** frame building; blasting demolition; subway tunnel; test monitoring; dynamic response; pore water pressure



**Citation:** Wang, W.; Xie, X.; Yuan, F.; Luo, P.; Wu, Y.; Liu, C.; Nie, S. Influence of a Frame Structure Building Demolition on an Adjacent Subway Tunnel: Monitoring and Analysis. *Buildings* **2024**, *14*, 3974. <https://doi.org/10.3390/buildings14123974>

Academic Editor: Luca Martinelli

Received: 6 November 2024

Revised: 5 December 2024

Accepted: 11 December 2024

Published: 14 December 2024



**Copyright:** © 2024 by the authors. Licensee MDPI, Basel, Switzerland. This article is an open access article distributed under the terms and conditions of the Creative Commons Attribution (CC BY) license (<https://creativecommons.org/licenses/by/4.0/>).

## 1. Introduction

As urbanization in China continues at a rapid pace, rail transit, such as subways and light rails, has become an increasingly integral component of the modern urban transportation network. At the present time, the most commonly employed method for the dismantling of large structures in complex urban environments is demolition by blasting. This method is becoming increasingly prevalent in projects situated in proximity to subway lines [1]. During the demolition process, the detonation of explosives and the impact load produced by the collapsing mass of the building have the potential to damage nearby underground structures and pipelines [2]. Furthermore, in the event that the tunnel is situated within saturated sandy soil, the impact load resulting from the building striking the ground may give rise to sudden fluctuations in pore pressure, which could have a detrimental impact on the integrity of subway tunnels. Subways represent a vital component of urban transportation, and it is therefore of the utmost importance to ensure the safety of operational subway tunnels during demolition projects in the vicinity.

Research into the dynamic response and damage patterns of subway tunnels under blast conditions has produced significant results both nationally and internationally. Scholars such as Jung et al. [3] have developed internal blast models with different explosive charges to analyze the displacement and velocity curves at the tunnel crown and lining and to study the propagation of shock waves inside tunnels. Jinshan Sun et al. [4,5] proposed a transient stress concept model to describe in detail the stress state of reinforced concrete

columns during the demolition of tall buildings. Researchers such as Guangdong Yang et al. [6] have considered complex processes such as explosive detonation, shock wave propagation, shock wave–structure interaction, and dynamic response of structures, and used the Lagrange–Euler coupling algorithm to study the damage process, spatial distribution, and failure modes of underwater tunnels under explosive impact loads. Gang Luo et al. [7] and others have studied the dynamic response and damage characteristics of subway tunnels under various conditions, such as different explosive weights, distances between the tunnel and the blast source, and the presence or absence of linings. Giannaros et al. [8] analyzed the blast vibration response of composite pipelines and concrete tunnels using the LS-DYNA dynamic finite element method. Jianwen Liu et al. [9] and others, based on Hertz’s nonlinear elastic contact theory, simulated the wheel–rail contact relationship, considering the spatial structural characteristics and mutual contact relationships of vehicles, tracks, tunnels, and surrounding rocks, and established an integrated vehicle–track–tunnel–surrounding rock calculation model to calculate the dynamic response of structures caused by train operation after deformation due to shield tunnel uplift caused by excavation. In their study, Ruishan Cheng and colleagues [10] presented the latest advancements in the fields of dynamic response, damage assessment, and damage mitigation of tunnels under explosive loads. Wang et al. [11] and others conducted research into the dynamic response characteristics of Metro Line 1 tunnels under train loads, taking into account different geological conditions and spatial structural features. Mohamed H. Mussa et al. [12] evaluated the safety of tunnels based on the weight of explosives, tunnel lining thickness, and burial depth using a single degree of freedom method, demonstrating the stability of the tunnels. Yubing Yang et al. [13] and others employed the finite element software ANSYS/LS-DYNA to analyze the dynamic response of subway tunnels in soft soil foundations. This involved the detailed examination of the propagation of explosive stress waves through soil and tunnels, with a particular focus on the evaluation of the safety of tunnel linings based on failure criteria. In urban subway tunnel blasting excavation projects, ensuring the safety of surface buildings (structures) in the crossing area is a key concern. Zhaotun An et al. [14] studied the time-varying behavior of damaged gas pipelines under the impact of falling objects and found that a certain level of internal pressure is beneficial for protecting PE pipelines. Huabing Zhao et al. [15] conducted a numerical simulation study on the dynamic response of subway tunnels under the impact load of a bridge collapse. Based on the results, they further optimized the protective system, safeguarding the subway tunnels from damage. Feng Yang et al. [16] studied the effects of explosions on concrete pipelines with different types of joints. They provided recommendations for the protection, repair, and failure identification of segmented structures under explosive conditions. Nan Jiang et al. [17] combined field tests and the existing literature to analyze the dynamic response patterns of shallow-buried pipelines under the influence of blasting vibrations and highlighted the frontiers and key areas of related research. Yu et al. [18] developed an integrated computational model to analyze the response of tunnel–soil–structure systems under seismic conditions. The study revealed that the presence of subway tunnels can cause an acceleration peak amplification zone within a certain range on the ground surface. Charlie et al. [19] studied the changes in excess pore pressure and liquefaction phenomena induced by explosive loads in large saturated sandy soils and developed an empirical relationship applicable to single charge detonations. Zhan et al. [20] investigated the response of pore water pressure and the liquefaction of soil under high-frequency pile driving vibration loads. Many existing studies focus on specific elements such as vibration or pore water pressure but rarely consider multiple dynamic responses simultaneously. Furthermore, most research has been conducted in isolated or regulated environments, and comprehensive control measures to mitigate adverse effects in complex environments are lacking. This disparity poses a significant barrier to the development of safe and efficient demolition designs in densely populated urban areas, where the interactions between buildings and varying ground conditions add complexity to the blasting operation.

The impact load of the building collapse and the explosive load generation mechanism are different, which may have a more significant impact on the surrounding underground structure. In this paper, based on the blasting and demolition project of a frame structure building adjacent to an underground tunnel, the blasting and demolition technology of reserving buffer floors is adopted, and a comprehensive monitoring study of the adjacent underground tunnel is carried out. Through blast vibration, dynamic strain, deformation and settlement, pore water pressure and other monitoring means, the structural response characteristics of the underground tunnel are analyzed from various perspectives, and the impact of blasting and demolition of the building on the adjacent underground tunnel is evaluated. This study provides an important theoretical basis and practical guidance for the impact of blasting and demolition on underground structures in complex urban environments.

## 2. Project Introduction

The building to be demolished is located in Jiangnan District, Wuhan City, China. It is an eight-story frame building, 62.5 m long, 9.0 m wide, and 27.3 m high. The minimum distance from the underground tunnel is 18 m, the tunnel depth is 16.7 m, the buried soil layer is mainly composed of silt, clay, and silty clay, and the groundwater table is high. The spatial location of its underground tunnel is shown in Figure 1. In order to minimize the impact of the collapsed body on the underground tunnel, the overall blasting program was designed with a ‘westward directional blast’.

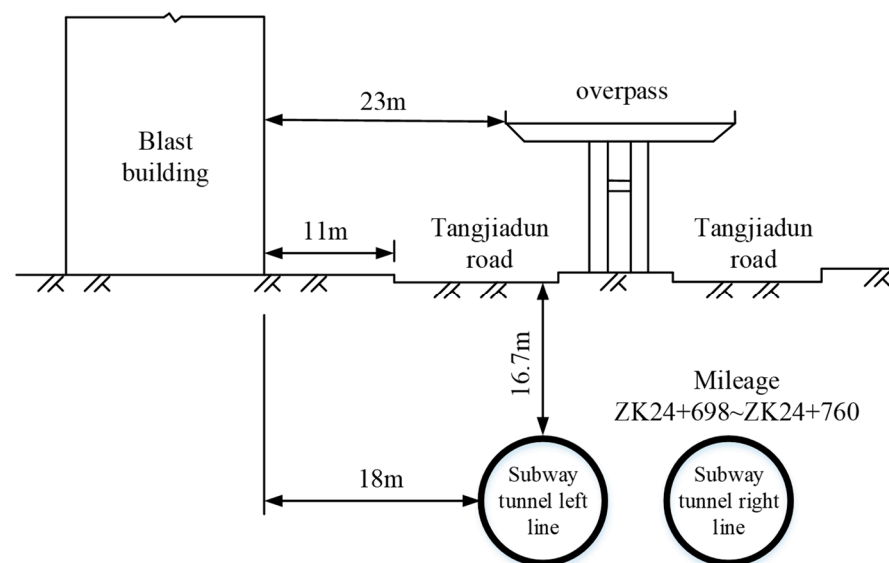


**Figure 1.** Position relationship between the building and the subway tunnel (unit: m).

A total of 724 detonators were employed in the blasting operation. In the section extending from axis ① to axis ⑨ (to the south of the expansion joint), blasting cuts were placed on the second, third, and fourth floors. In the section extending from axis ⑩ to axis ⑱ (north of the expansion joint), blasting cuts were arranged on the second and third floors. The detonation proceeded in stages, commencing from the center and progressing in an outward, layer-by-layer manner. The first floor, which served as a buffer during the collapse, was blasted at 8000 ms. Figure 2 illustrates the schematic diagram of the blasting cuts, and Table 1 provides a detailed account of the detonation times.

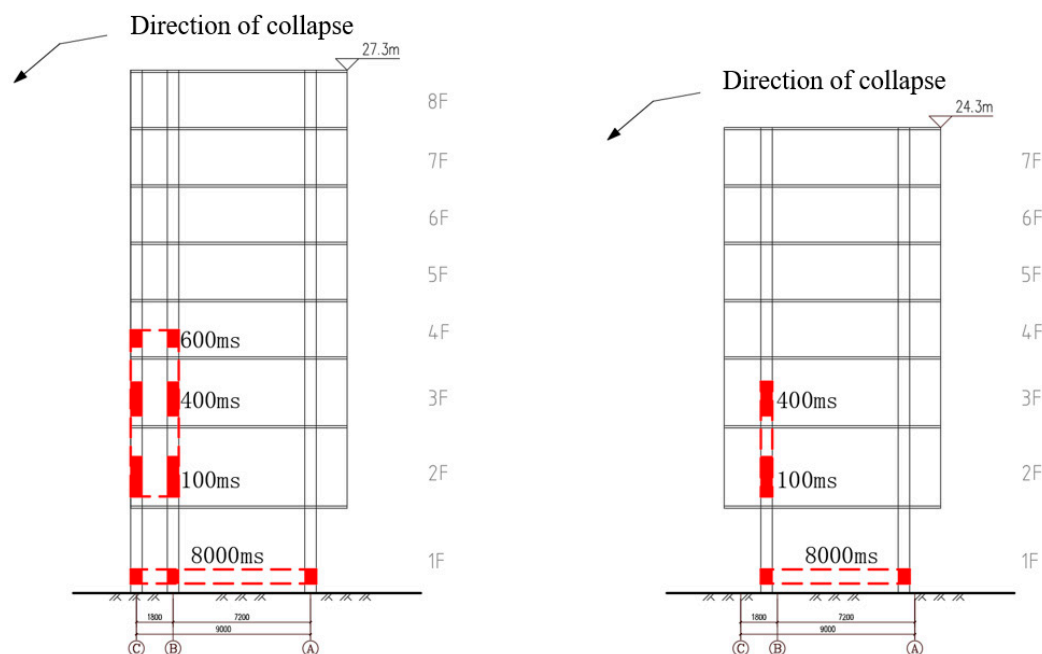


Figure 2. Blasting cut of mechanical edifice (unit: mm).

Table 1. Detonation time of blasting cut.

Axis Floor	Unit: Ms												
	1	2	3	4~5	6~7	8~9	9~10	11~12	13~14	15	16	17	
4F	2500	2000	1500	1000	800	600							
3F	2300	1800	1300	800	600	400	400	600	800	1300	1800	2300	
2F	2000	1500	1000	500	300	100	100	300	500	1000	1500	2000	
1F								8000					

### 3. Monitoring Plan

#### 3.1. The Monitoring of Blast Vibration

The vibration monitoring equipment utilizes the Micromate vibration meter from INSTANTEL, Canada. The device's main technical specifications are as follows: (1) vibration range: 254 mm/s; (2) vibration resolution: 0.00788 mm/s; (3) vibration linearity accuracy: The device has a vibration range of  $\pm 0.5$  mm/s, a frequency range of 2–250 Hz, and a sampling rate of programmable switching at 1024, 2048, or 4096 Hz per channel. Six monitoring points are set up, all positioned on the side of the subway station and tunnel nearest to the blasting site. This setup allows for the collection of vibration data in three dimensions: horizontal and vertical. During the installation of the sensors, their orientation is adjusted to ensure that the x-direction points towards the center of the blast. It is also crucial to ensure that the medium or foundation surface where the sensors are mounted is free from contamination. High-strength, quick-setting gypsum is used for leveling the installation spot, ensuring that the velocity sensors are securely fixed. A schematic of the monitoring point locations is shown in Figure 3.



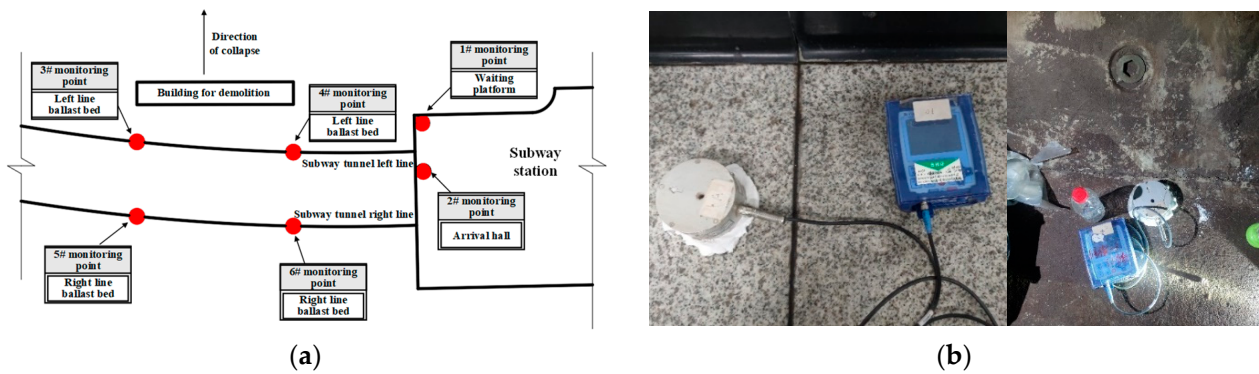


**Figure 3.** Vibration monitoring point layout: (a) Vibration monitoring point layout; (b) On-site layout of hall and track bed.

### 3.2. The Monitoring of Dynamic Strain

Dynamic strain monitoring is a technology that measures the strain produced by an object in response to external forces. It uses strain gauges attached to the surface of an object to convert strain into electrical signals for monitoring purposes. To monitor the dynamic response characteristics of the tunnel segments during the demolition and collapse process, DH8302 dynamic strain gauges and BX120-80AA concrete strain gauges were used with a sampling frequency of 5 kHz and a resolution of  $1 \mu\epsilon$ .

All dynamic strain monitoring points on the segments are located on the left tunnel. The configuration consists of three sections with a total of twelve strain gauges distributed over six monitoring points. The aforementioned strain gauges are located at the tunnel haunches, which correspond to the center and the two ends of the structure being demolished. This is shown in Figure 4. Each monitoring point is equipped with two strain gauges, one circumferential and one axial, on the surface of the tunnel segment. The gauges allow real-time observation of the dynamic strain on the segments at the moment of collapse.

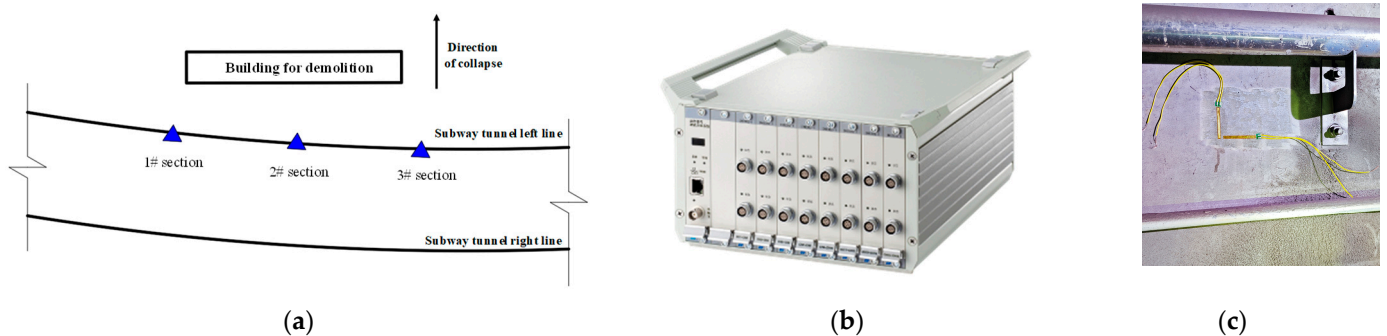


**Figure 4.** Segment dynamic strain monitoring record: (a) Monitoring section layout; (b) DH8302 type dynamic strain gauge; (c) Strain gauge site layout.

### 3.3. The Monitoring of Displacement and Settlement

The most intuitive manifestations of the effects of blasting in underground tunnels are displacement and settlement changes. Therefore, deformation and settlement monitoring is carried out inside the metro tunnel using a three-dimensional scanner to scan the interior of the tunnel, collect tunnel cloud data, and compare the two conditions before and after blasting. The scan results evaluate the internal deformation and roundness of the tunnel, and the measurement points and observation methods are shown in Figure 5.

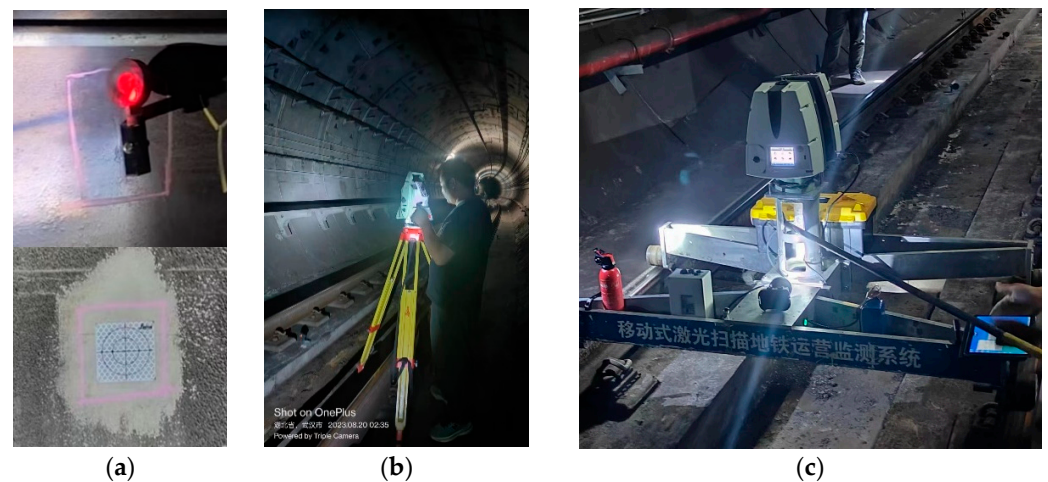


**Figure 5.** Tunnel deformation and settlement monitoring records: (a) Monitoring point mark; (b) Section monitoring point records; (c) Tunnel 3D laser scanning.

The Swiss Leica TM30 total station measured horizontal displacement, while the DNA03 digital level assessed settlement. The RIEGL VZ-400i three-dimensional laser scanner analyzed tunnel deformation. Comparative observations were made five times at key points within the metro station, track bed, and tunnel segments before and after blasting.

The tunnel comprised 28 monitoring sections: 5 on the right track and 23 on the left. The monitored area under the demolished building was 5 m in depth and extended 50 m in both directions. Sections within this extended area were spaced 10 m apart. Each section included deformation monitoring points at the base, arch waist, and vault.

### 3.4. The Monitoring of Pore Water Pressure and Displacement

The impact load from a building collapsing onto the ground causes sudden changes in pore water pressure. Faster changes lead to more pronounced pressure spikes, creating compression waves at the pressure change interface. During this process, the compressed pore water can erode and compress the foundation, potentially impacting the subway tunnel. Therefore, monitoring pore water pressure is essential.

Drilling between the demolished building and the subway tunnel could damage shallow pipe networks, roads, viaducts, and structures. To avoid this, three monitoring points will be placed evenly along the longitudinal axis near the east side of the demolished building, as shown in Figure 6. The boreholes are located approximately 16 m from the boundary of the subway line and 2–3 m from the building.

Monitoring is carried out using KYJ30 steel-string pore water pressure gauges and 200 kPa manometers, with the ZXY-2 steel-string frequency receiver recording frequency data. The frequency measurements are then converted to pore water pressure values. As groundwater stabilization takes time, the first sensor reading is taken 12 h after installation, with follow-up measurements taken after blasting and completion.

As shown in Figure 7, horizontal displacement is monitored using an inclinometer system consisting of fiber Bragg grating (FBG) sensors, flexible deformation tubing, and rigid PVC tubing. The flexible and rigid pipes are installed alternately along the monitoring line, with the FBG sensors embedded in the flexible pipes. The bottom PVC segment is fixed and calibrated to set the initial zero displacement. The changes in tilt angle recorded by the FBG sensors are used to calculate the deformation at each sensor location.

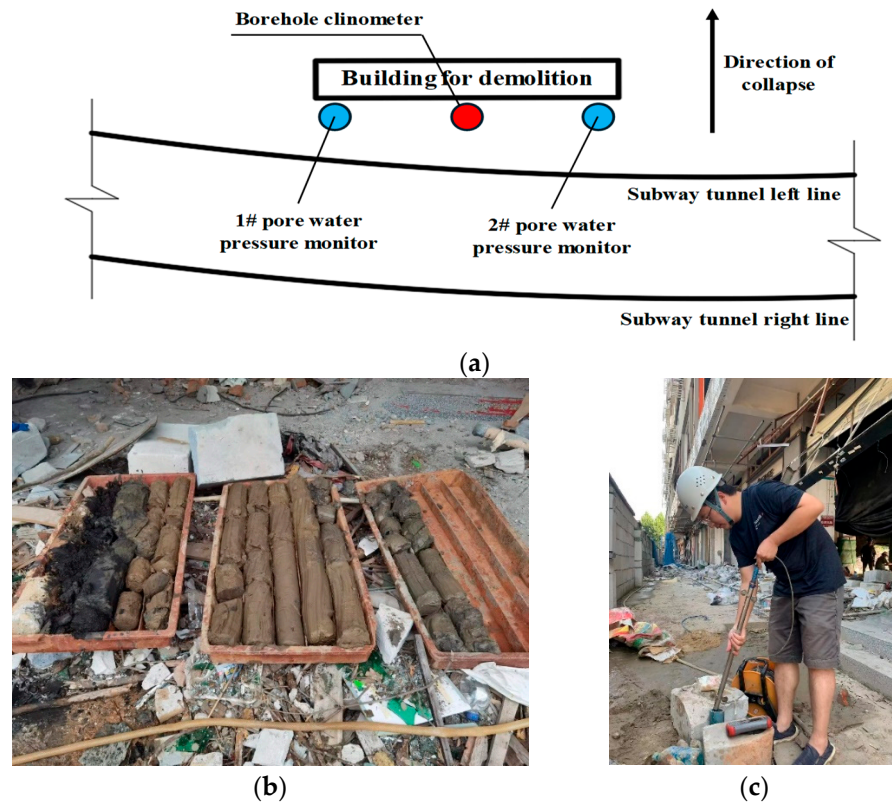


**Figure 6.** Pore water pressure and displacement monitoring records: (a). Monitoring point layout; (b) Equipment placement hole coring; (c). Installation of pore water pressure gauge.

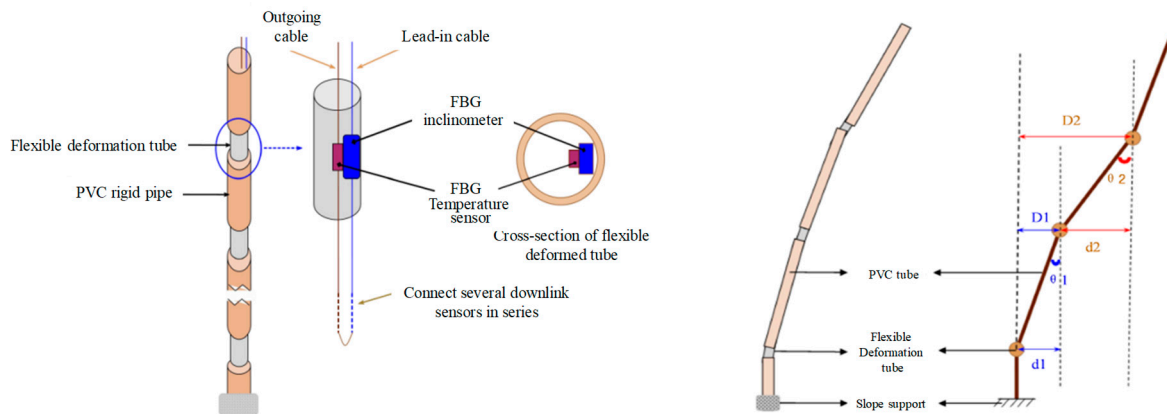


**Figure 7.** Incliner principle.

## 4. Analysis of Impact Monitoring Results of Building Blasting and Collapse

### 4.1. Analysis of Blasting Vibration Characteristics

The analysis of the monitoring results focuses on the impact of blast vibration on buildings, which is primarily caused by the propagation of vibration waves from the explosion through the ground to the structures. The collected vibration data show that the total duration of vibrations during the building demolition was approximately 10.3 s.

The vibration response of the subway tunnel during demolition can be divided into four distinct phases: the blast cut formation phase, the blast cut closure phase, the contact phase between the collapsing structure and the ground, and the secondary disintegration phase of the structure. Figures 8 and 9 illustrate these phases in detail.

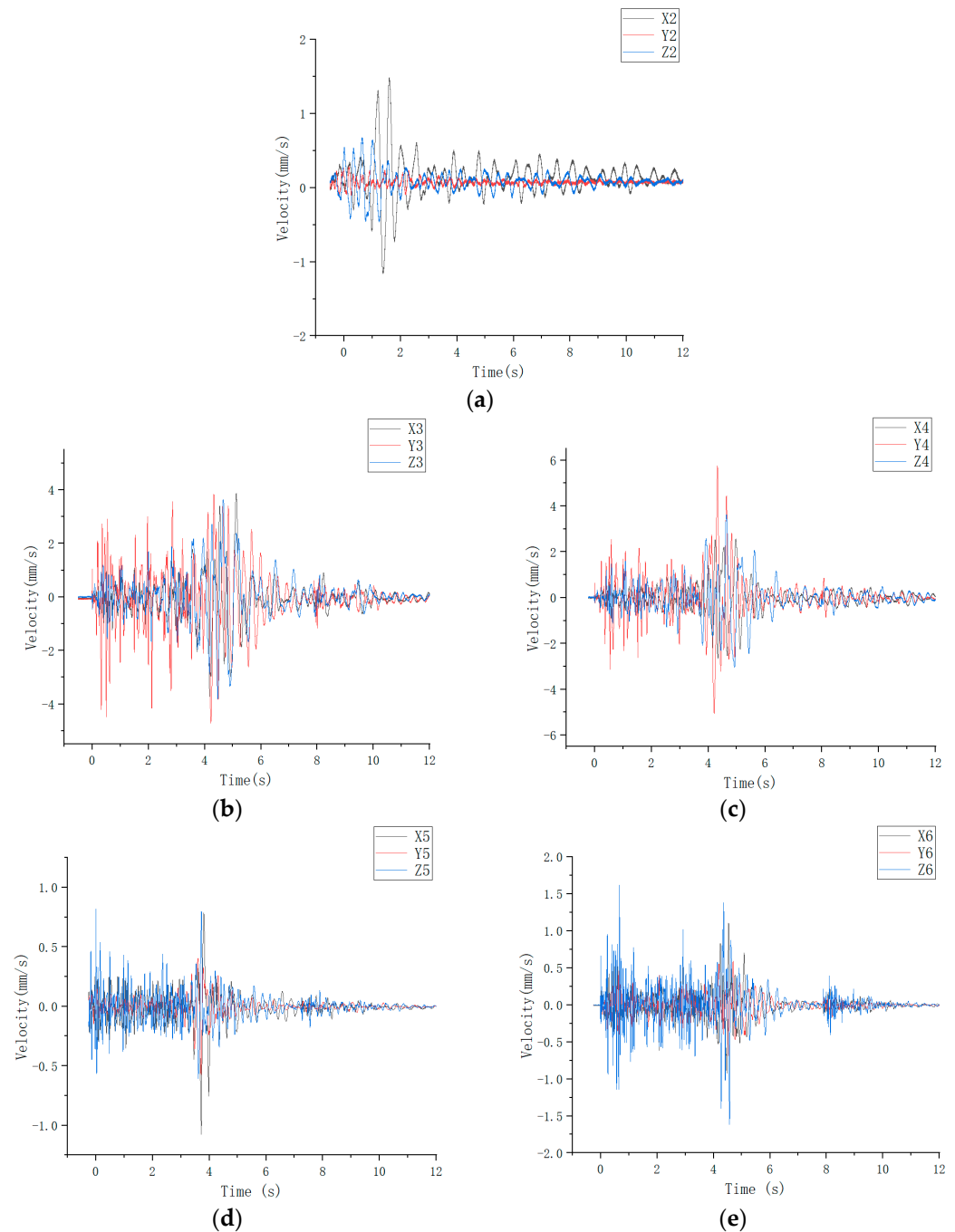


**Figure 8.** Vibration speed of each measuring point: (a) 2# vibration speed; (b) 3# vibration speed; (c) 4# vibration speed; (d) 5# vibration speed; (e) 6# vibration speed.

1. From 0.00 s to 2.50 s: The vibration response corresponds to the timing of column detonations within the blast cuts. Between 0.00–0.80 s and 1.50–2.30 s, concentrated column detonations produced higher particle vibration velocities. Peak values were recorded at 0.50 s (4.46 mm/s) and 2.12 s (4.12 mm/s).
2. At 2.80 s: At this time, monitoring at point #3 recorded a peak particle vibration velocity of 3.46 mm/s. The unstable collapse analysis of the building indicates that this moment corresponds to the closure of the upper blast cut, with the buffer cut engaging and rapidly reducing the particle vibration velocity.
3. From 4.00 s to 7.50 s: During this period, the subway tunnel experienced a peak vibration velocity of 5.74 mm/s. This phase corresponds to the directed overall



- collapse of the building, where the structure made full contact with the ground and began to disintegrate. Vibration levels gradually stabilized as the collapse progressed.
- At 8.00 s: Following the complete detonation of the buffer section, the particle vibration rate increased to 1.17 mm/s, followed by approximately 2.3 s of oscillation before stabilizing. By this time the building had been completely demolished, marking the end of the demolition process.

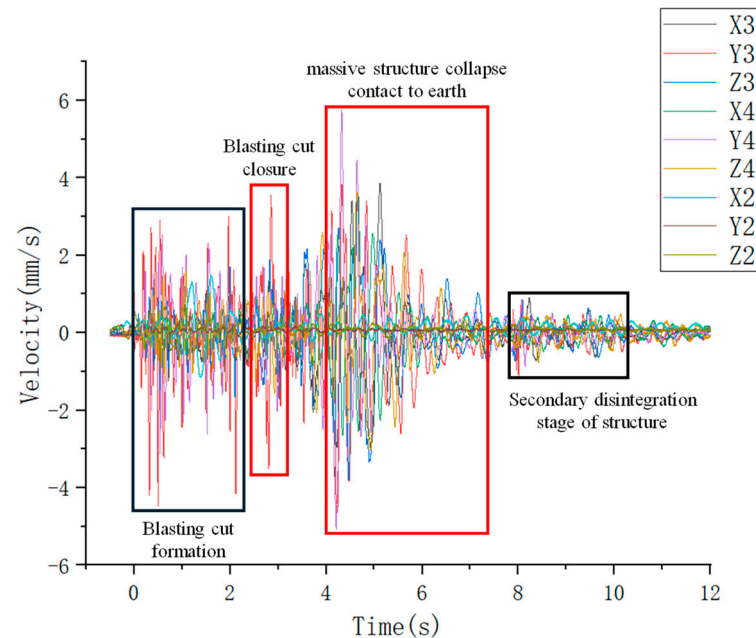


**Figure 9.** Vibration velocity result division.

The monitoring point closest to the blast site, known as Point 4, recorded the highest peak vibration velocity of 0.57 cm/s. This value is well below the safety threshold for underground tunnels (1.5 cm/s) specified in the Blasting Safety Regulations (GB6722-2014) [21] and the Technical Specifications for Structural Safety Protection of Urban Rail Transit (CJJ/T 202-2013) [22]. Therefore, the vibrations generated during the demolition are unlikely to affect the subway tunnel or its internal electrical systems.

#### 4.2. Analysis of Dynamic Response Characteristics of Tunnel Segments

The results of the dynamic strain monitoring, shown in Figure 10, indicate that during demolition and collapse, the tunnel segments mainly experienced circumferential tension and compression, eventually returning to their original equilibrium values. This behavior confirms that the deformation remained within the elastic range. From 4.0 to 7.0 s, the most significant dynamic strain occurred as the building came into contact with the ground during the overall collapse. The greatest impact on the tunnel segments was observed in section #2, closest to the blast center.

The maximum tensile and compressive strains were recorded in section #2. On the left side, the peak circumferential tensile strain reached  $7.1 \mu\epsilon$ , corresponding to a tensile stress of 0.245 MPa, while the peak axial compressive strain was  $-10.5 \mu\epsilon$ , corresponding to a compressive stress of 0.362 MPa. On the right, the peak circumferential tensile strain was  $9.4 \mu\epsilon$ , corresponding to a tensile stress of 0.324 MPa, while the peak axial compressive strain was  $-5.1 \mu\epsilon$ , corresponding to a compressive stress of 0.176 MPa.

The calculated peak dynamic tensile stress for the tunnel segments was 0.33 MPa, and the peak dynamic compressive stress was 0.36 MPa. According to the Code for Design of Concrete Structures (GB50010-2010) [23], the axial compressive strength of C50 concrete is 23.1 MPa, and the axial tensile strength is 1.89 MPa. Therefore, the demolition and collapse of the building do not pose a threat to the structural integrity of the underground tunnel segments.

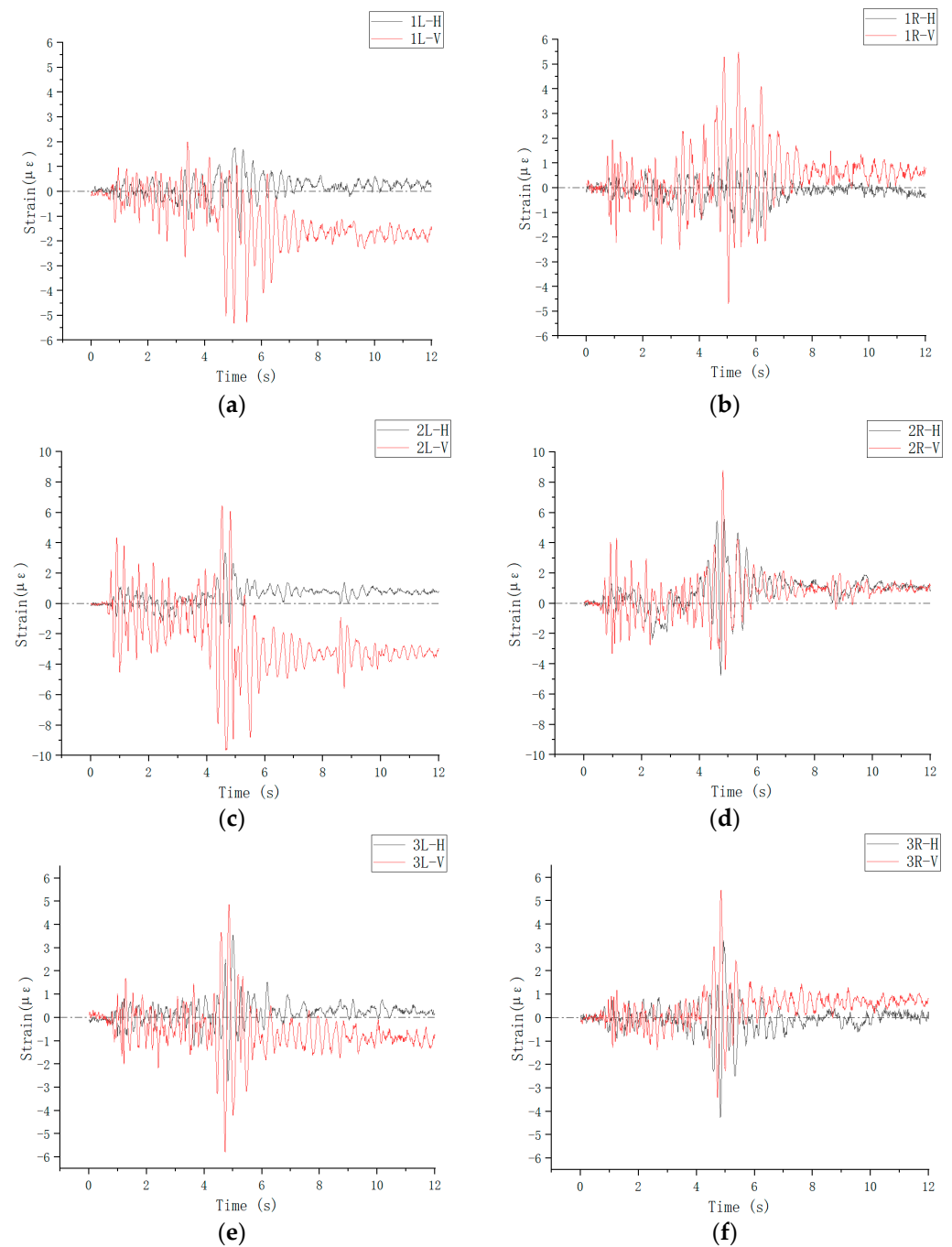


**Figure 10.** Dynamic strain of each measuring point: (a) 1# left strain; (b) 1# right strain; (c) 2# left strain; (d) 2# right strain; (e) 3# left strain; (f) 3# right strain.

#### 4.3. Analysis of Deformation and Settlement

Once the monitoring points had been established, an initial measurement was taken using the appropriate equipment. This baseline measurement was compared with data collected at three subsequent intervals: immediately after blasting, 3 days after blasting, and 7 days after blasting. The cumulative displacement changes in the tunnel segments were recorded, and the peak values were extracted and plotted as shown in Figure 11.



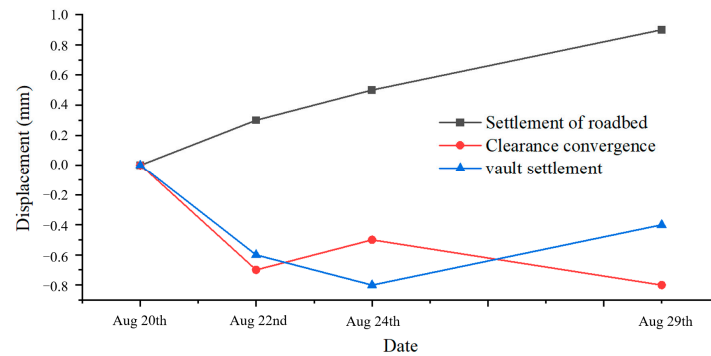


**Figure 11.** Peak displacement variation diagram.

The four sets of observational data gathered before and after the blasting indicate that the displacement changes at each monitoring point within the left and right lines of the subway tunnel were all less than 1 mm. This level of displacement is in compliance with the standards and guidelines set forth in the “Blasting Safety Regulations” (GB6722-2014) and the “Technical Specifications for Structural Safety Protection of Urban Rail Transit” (CJJ/T202-2013), as well as established protection cases.

#### 4.4. Analysis of Pore Water Pressure and Displacement

Pore water pressure was monitored at regular intervals before, during, and after the blasting operations, and the results are shown in Figure 12.

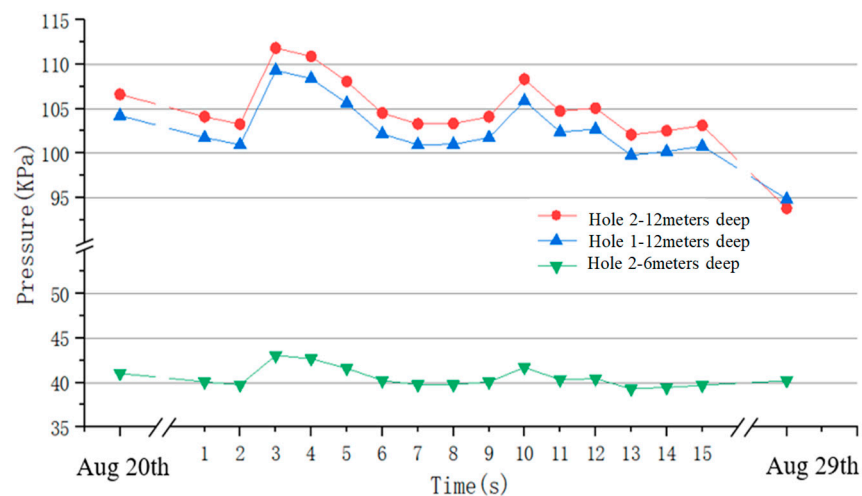


**Figure 12.** Pore water pressure changes.

Vibration changes the density of the soil structure, affecting pore water flow paths and permeability, which can lead to local redistribution of pore water pressure. Measurements show that at a depth of 12 m the peak pore water pressure reached 111.83 kPa, while the lowest recorded value was 99.78 kPa. These changes were significantly influenced by the blast vibrations and showed a certain time lag, with more pronounced effects in deeper soil layers. During the collapse of the building, variations in pore water pressure were observed in the soil from the surface to a depth of 12 m, on the east side of the blast zone. However, these variations were relatively small, with the maximum increase not exceeding 7 kPa. The pore water pressure quickly returned to its initial state after the blast was completed.

A comparison of the pore water pressure values before and one week after the blast showed a decrease to 93.82 kPa. This reduction is primarily due to the proximity of the monitoring point to the building, where surface loads have a significant effect on pore water pressure. As the blasting was completed and the subsequent fragmentation and

removal of debris progressed, the surface load decreased with a corresponding decrease in pore water pressure.

Inclinometer monitoring data, shown in Figure 13, indicate minimal horizontal displacement in the deep soil layers before and after blasting, with displacements not exceeding 0.5 mm.

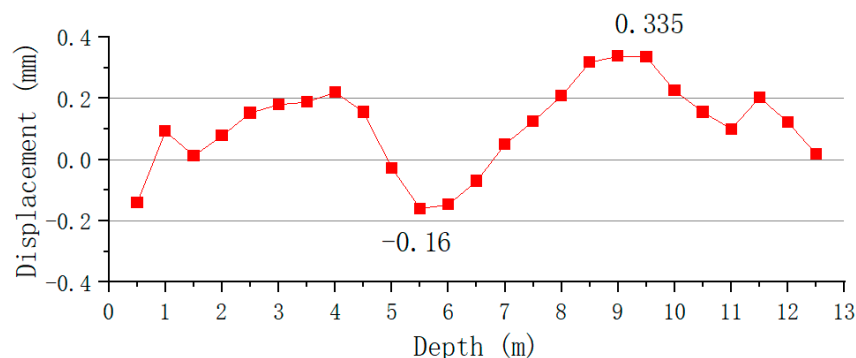


Figure 13. Horizontal displacement changes with depth.

### 5. Blast Effect

As shown in Figure 14, the mechanical edifice collapsed in approximately 6.80 s. The cutting on the first floor was detonated at 8.00 s, resulting in a secondary disintegration of the building with sufficient fragmentation. The height of the muck pile was about 6.7 m, and there was basically no recoil. The monitored particle vibration velocities at the surrounding protected objects were all within the allowable safety range of the specifications. All indicators within the adjacent subway tunnel were also within the safety range. During the process, no damage was caused to the surrounding building facilities and the adjacent subway tunnel. The situation of the muck pile is shown in Figure 15.

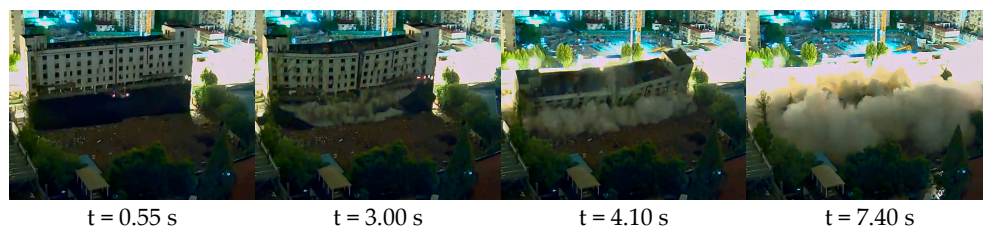


Figure 14. The collapse process of the mechanical edifice.



Figure 15. The muck pile of mechanical edifice.

### 6. Conclusions

This paper integrates a range of monitoring techniques, including blast vibration tests, dynamic strain tests on tunnel segments, deformation and settlement tests, and pore water

pressure and displacement tests, to provide a comprehensive analysis of the impact of the demolition of a frame building on the nearby metro tunnel. The following conclusions and recommendations can be drawn from the data presented.

- (1) By analyzing the vibration signals, the vibration waveform is divided into four distinct stages, corresponding to short-duration, high-frequency blast-induced vibrations and long-duration, low-frequency ground impact vibrations. These stages collectively characterize the entire evolutionary process of building demolition and ground impact. The blast-induced vibrations have a significant effect on the pore water tension, while the ground-impact vibrations have a more pronounced effect on the structural integrity of the subway tunnel.
- (2) The deformation of the subway tunnel segments in response to the total collapse of the building was predominantly characterized by circumferential tension and compression, all within the elastic range. During the 4.0 s to 7.0 s period, it was observed that the segments exhibited significant additional dynamic strain, which eventually returned to their original equilibrium values.
- (3) The change in pore water pressure was significantly influenced by the blast vibrations, especially in the deeper soil layers, with a certain delay. During the collapse of the building, the increase in pore water pressure in the soil between the building and the metro tunnel did not exceed 7 kPa. In addition, the pressure quickly decreased to near-initial values after the blast, ensuring that it did not adversely affect the dynamic response of the metro tunnel.
- (4) Following the complete demolition of the building, all monitoring results were found to be within safe control standards. The use of techniques such as “raising the blast cut position, using the lower floors as a vibration damping buffer layer, and staggering the detonation floor by floor” effectively dispersed the mass of the building touching the ground simultaneously, significantly reducing the impact load of the building collapse. The monitoring system used in the thesis provides insights that will be valuable in similar demolition projects near underground tunnels.

**Author Contributions:** Conceptualization, W.W. and X.X.; methodology, W.W.; software, C.L.; validation, W.W., F.Y. and P.L.; formal analysis, F.Y.; investigation, Y.W.; resources, S.N.; data curation, F.Y.; writing—original draft preparation, F.Y.; writing—review and editing, W.W. All authors have read and agreed to the published version of the manuscript.

**Funding:** This research received no external funding.

**Data Availability Statement:** The original contributions presented in this study are included in the article. Further inquiries can be directed to the corresponding author.

**Conflicts of Interest:** Authors Wei Wang, Xianqi Xie, Peng Luo, Yue Wu and Changbang Liu were employed by the company Wuhan Explosions & Blasting Co., Ltd. The remaining authors declare that the research was conducted in the absence of any commercial or financial relationships that could be construed as a potential conflict of interest.

## References

1. Xie, X. Precision blasting, current status and its prospective. *Strateg. Study CAE* **2014**, *16*, 14–19. (In Chinese)
2. Xie, X. Development situation and trend of demolition blasting technology. *Blasting* **2019**, *36*, 1–12. (In Chinese)
3. Jung, H.J.; Eem, S.H.; Jang, D.D. Dynamic response of tunnel under different explosion equivalents. *Soil Dyn. Earthq. Eng.* **2011**, *22*, 1439–1450.
4. Sun, J.; Jia, Y.; Yao, Y.; Xie, X. Experimental investigation of stress transients of blasted RC columns in the blasting demolition of buildings. *Eng. Struct.* **2020**, *210*, 110417. [[CrossRef](#)]
5. Sun, J.; Jia, Y.; Xie, X.; Yao, Y. Design criteria for the folding implosion of high-rise RC buildings. *Eng. Struct.* **2021**, *233*, 111933. [[CrossRef](#)]
6. Yang, G.; Wang, G.; Li, Q. Dynamic response and damage patterns of underwater tunnel subjected to blast loads. *J. Vib. Shock* **2022**, *41*, 150–158. (In Chinese)
7. Luo, G.; Zhang, Y.; Ren, Y.; Guo, Z.; Pan, S. Dynamic response analysis of submerged floating tunnel subjected to underwater explosion-vehicle coupled action. *Eng. Mech.* **2021**, *38*, 109103. [[CrossRef](#)]

8. Giannaros, E.; Kotzakolios, T.; Kostopoulos, V. Blast response of composite pipeline structure using finite element techniques. *J. Compos. Mater.* **2016**, *50*, 3459–3476. [[CrossRef](#)]
9. Liu, J.; Shi, C.; Lei, M. Dynamic response of subway shield tunnel structure under differential deformation. *J. Vib. Acoust.* **2021**, *40*, 212–220. (In Chinese)
10. Cheng, R.; Chen, W.; Hao, H.; Li, J. A state-of-the-art review of road tunnel subjected to blast loads. *Tunn. Undergr. Space Technol.* **2021**, *112*, 103911. [[CrossRef](#)]
11. Wang, D.; Luo, J.; Li, F.; Wang, L.; Su, J. Research on dynamic response and fatigue life of tunnel bottom structure under coupled action of train load and groundwater. *Soil Dyn. Earthq. Eng.* **2022**, *161*, 107405. [[CrossRef](#)]
12. Mussa, M.H.; Mutalib, A.A.; Hamid, R.; Naidu, S.R.; Radzi, N.A.M.; Abedini, M. Assessment of damage to an underground box tunnel by a surface explosion. *Tunn. Undergr. Space Technol.* **2017**, *66*, 64–76. [[CrossRef](#)]
13. Yang, Y.; Xie, X.; Wang, R. Numerical simulation of dynamic response of operating metro tunnel induced by ground explosion. *J. Rock Mech. Geotech. Eng.* **2010**, *2*, 373–384.
14. An, Z.; Tang, Q.; Huang, Y.; Li, H. Time-dependent analysis of buried high-density polyethylene (PE100) pipelines with a scratch defect subjected to touchdown impact loading of blasting collapsed body. *Int. J. Press. Vessel. Pip.* **2022**, *195*, 104605. [[CrossRef](#)]
15. Zhao, H.; Long, Y.; Ji, C.; Li, X.; Zhong, M. Study on the dynamic response of subway tunnel by viaduct collapsing vibration and the protective measures of reducing vibration. *J. Vibroeng.* **2015**, *17*, 2433–2443.
16. Yang, F.; Jia, J.; Jiang, N.; Zhou, C.; Luo, X.; Lyu, G. Damage and deformation behavior of reinforced concrete pipes with varying joints under surface explosion. *Eng. Fail. Anal.* **2024**, *156*, 107817. [[CrossRef](#)]
17. Jiang, N.; Zhu, B.; Zhou, C.; Li, H.; Wu, B.; Yao, Y.; Wu, T. Blasting vibration effect on the buried pipeline: A brief overview. *Eng. Fail. Anal.* **2021**, *129*, 105709. [[CrossRef](#)]
18. Yu, J.; Wang, Z.Z. The dynamic interaction of the soil-tunnel-building system under seismic waves. *Soil Dyn. Earthq. Eng.* **2021**, *144*, 106686. [[CrossRef](#)]
19. Charlie, W.A.; Bretz, T.E.; Schure, L.A.; Doehring, D.O. Blast-induced pore pressure and liquefaction of saturated sand. *J. Geotech. Geoenviron. Eng.* **2013**, *139*, 1308–1319. [[CrossRef](#)]
20. Zhan, J.; Chen, J.; Wang, W.; Li, M. In situ investigation on pore-water pressure response during vibratory pile driving with high frequency. *Acta Geotech.* **2024**, *19*, 2649–2668. [[CrossRef](#)]
21. GB6722-2014; Safety Regulations for Blasting. Standards Press of China: Beijing, China, 2014.
22. CJJ/T202-2013; Technical Code for Protection Structures of Urban Rail Transit. China Architecture Publishing & Media Co., Ltd.: Beijing, China, 2014.
23. GB50010-2010; Code for Design of Concrete Structures. China Architecture Publishing & Media Co., Ltd.: Beijing, China, 2010.

**Disclaimer/Publisher's Note:** The statements, opinions and data contained in all publications are solely those of the individual author(s) and contributor(s) and not of MDPI and/or the editor(s). MDPI and/or the editor(s) disclaim responsibility for any injury to people or property resulting from any ideas, methods, instructions or products referred to in the content.